Applied Surface Science 636 (2023) 157807

Contents lists available at ScienceDirect

Applied Surface Science

journal homepage: www.elsevier.com/locate/apsusc

Full Length Article

Porphyrin central metal ion driven self-assembling in heterogeneous ZnTPP – CoTPP films grown on Fe(0 0 1)-$p(1 \times 1)$O

Isheta Majumdar *, Francesco Goto, Alberto Calloni, Guglielmo Albani, Lamberto Duò, Marco Finazzi, Franco Ciccacci:, Gianlorenzo Bussetti

Department of Physics, Politecnico di Milano, Piazza Leonardo da Vinci 32, 20133 Milan, Italy

ARTICLE INFO

Keywords:
Metal tetraphenylporphyrins
Self-assembling
Ultra-thin metal oxide layers
Fe(0 0 1)-$p(1 \times 1)$O
PES
LEED

ABSTRACT

Metal tetraphenylporphyrins (MTPPs, with M = Zn, Co) deposited on an oxygen-passivated Fe substrate, namely Fe(0 0 1)-$p(1 \times 1)$O, were studied to understand the mechanism of molecular self-assembling on ultrathin metal-oxide films. These were characterized by photoemission spectroscopy (PES) and low energy electron diffraction (LEED). Heterogeneous MTPP monolayers (ZnTPP + CoTPP) were grown at room temperature by depositing a sub-monolayer of ZnTPP on Fe(0 0 1)-$p(1 \times 1)$O followed by a sub-monolayer of CoTPP or vice-versa, or by co-deposition.

Homogeneous layers are characterized by markedly different molecular superstructures, as shown by LEED. Conversely, heterogeneous monolayers reflected an even more complex behavior: in particular, it was observed that the deposition of a small amount of CoTPP before or simultaneous to the dosing of ZnTPP molecules was able to stabilize a (5×5)R37° diffraction pattern, characteristic of homogeneous CoTPP, whereas homogeneous ZnTPP layers are associated to a straight (5×5) one. The observed differences in the ordering of the molecular self-assembling as a consequence of combining the two MTPPs highlights a significant influence of one MTPP over the other depending upon the central metal ion and not upon the molecular skeleton.

1. Introduction

The field of organic electronics has seen the emergence of engineered hybrid metal electrode/organic molecule interfaces where molecules can be ordinally assembled in 2D scalable devices [1]. In this regard, many compounds have been synthesized and studied to obtain specific properties at the interface [2]. Organic molecules can also be functionalized, and radical groups can be bound to the main molecular structure ensuring a change in the physical/chemical properties of the compounds [3]. Considering the emergency of realizing hybrid devices, where electronic charge transport properties can be fine-tuned, in-depth investigations of the inorganic/organic interface constitute an ongoing and ambitious research theme [4–10].

The development of complete organic devices poses a generic challenge, which is, to preserve chemical, physical and electronic properties when organic molecules are placed onto a substrate (e.g. metallic) due to a mutual interaction between the molecules and the substrate. In this regard, metal surfaces passivated by single atomic layers of oxygen called ultra-thin metal oxide layers have been proposed to have the proper requisites in view of preserving the electronic properties of the chosen molecules. One such substrate is Fe(0 0 1)-$p(1 \times 1)$O, where a single layer of oxygen atoms are located at the four-fold symmetrical "hollows" of the substrate Fe(0 0 1) surface [11,12]. The reason for using ultra-thin iron oxide resides in the fact that the properties of the Fe substrate itself are exploitable such as that of its conductivity and ferromagnetism. But since the bare Fe substrate is highly interactive, there is the need for a decoupling layer between the metal substrate and the organic molecules to be deposited. Graphene has been also proposed to act as a well-functioning decoupling layer, e.g. on Ni [13]. However, the orthohexagonal lattice structure of graphene is not compatible with the body centered cubic lattice structure of iron crystal. A standard ultra-thin Fe(0 0 1)-$p(1 \times 1)$O layer prepared by following a surface oxygen passivation protocol outlined in the Material and Methods section, has already been established by the authors to be able to efficiently decouple the deposited organic molecules, which retain their compositional integrity and a minimally perturbed electronic structure w.r.t the

* Corresponding author.
E-mail address: isheta.majumdar@polimi.it (I. Majumdar).

https://doi.org/10.1016/j.apsusc.2023.157807
Received 17 March 2023; Received in revised form 9 June 2023; Accepted 15 June 2023
Available online 17 June 2023

freestanding case [14–18].

The organic material, metal tetraphenylporphyrin (MTPP) is composed of an almost flat tetra-pyrrolic macrocycle. At the skeleton border, four phenyl groups are linked to the main cavity of the molecule. A metal ion (in this case Zn^{2+} and Co^{2+}) can be placed inside the central ring, and its presence can alter the characteristic electronic properties of the molecule. MTPPs have been chosen as the model organic material for our investigation since they can accommodate different metal ions inside a central cavity and preserve the main skeleton of the molecule [19]. This occurrence appears as a natural way of tuning the chemical, electronic and transport properties. ZnTPP and CoTPP, the two MTPP molecules used in our study, are easily synthesized and available commercially in their pure forms. In free porphyrin complexes, the d-orbitals of the metal ion splits in one degenerate and three non-degenerate energy levels (D_{4h} symmetry). In this configuration, the lowest (d_{xy}) and highest ($d_{x^2-y^2}$) energy molecular orbitals are confined to the molecular *xy* plane, while the other three orbitals (d_{xz}, d_{yz}, d_{z^2}) project out of the molecular plane ($d_{\perp}$). Period 4 transition metal ions, in which the $d_{\perp}$ orbitals are unoccupied, tend to form stronger covalent bonds because these unoccupied orbitals can engage in orbital interaction and electron transfer from the substrate [20].

In our previous works, we have extensively investigated the structural and electronic properties of homogeneous monolayers of ZnTPP and CoTPP molecules deposited on Fe(0 0 1)-*p*(1 × 1)O substrates in an ultra-high vacuum (UHV) environment, using organic molecular beam epitaxy (OMBE). The two molecular systems show a very long range order that can be appreciated also with low energy electron diffraction (LEED). In particular, ZnTPP and CoTPP monolayers are characterized by two different LEED superstructures: it was observed that ZnTPP molecules deposition exhibited a (5 × 5) ordered reconstruction, while the (5 × 5) reconstruction of CoTPP molecules is rotated by 37° (w.r.t the underlying Fe crystal lattice vector), called a (5 × 5)R37° reconstruction [17,21–23]. In Ref. [24], we conducted a detailed investigation of the thermodynamic driving force leading to the formation of the corresponding molecular superstructures exploiting Density Functional Theory (DFT), complemented by Scanning Tunneling microscopy (STM) and Near Edge X-Ray Adsorption Fine Structure (NEXAFS) spectroscopy. STM data and calculations reveal very similar local morphologies where molecules share the same azimuthal orientation with the nearest neighbors [24], irrespective of the central metal ion and the molecular superstructure, possibly due to an intermolecular interaction mainly driven by peripheral groups, which are the same for both ZnTPP and CoTPP. Surprisingly, the calculated adsorption energies of both ZnTPP and CoTPP, for all possible configurations revealed only moderate energy differences, and the exact driving force for the formation of the ZnTPP and CoTPP superstructures therefore remains unclear.

In addition, the role of temperature during film growth was checked in a wide experimental campaign where the substrate was kept at various temperatures from cryogenic (about −100 °C) to relatively high temperatures (about 50 °C) during the depositions. In all the prepared samples, the ZnTPP and CoTPP characteristic reconstructions were stable if the substrate temperature was changed, thus suggesting a prominent role of kinetic effects in a wide temperature range, including also room temperature.

In this work, we propose a strategy to provide novel experimental data and shed more light on this issue. Heterogeneous monolayers (combination of ZnTPP and CoTPP), as a result of sequential deposition or a co-deposition, were exploited to observe a possible influence of one type of porphyrin molecule on the reconstruction of the other, in view of giving new insights on the role of the central metal ion in molecular assembling.

2. Material and Methods

2.1. Sample preparation

Sample preparation began in a UHV system (base pressure in high 10^{-11} Torr) with growing a 400 nm thick Fe(0 0 1) film on a clean MgO(0 0 1) single crystal substrate, by means of OMBE. At this thickness, the deposited Fe behaves as bulk crystal [21]. Then we proceed with the Fe (0 0 1)-*p*(1 × 1)O preparation by exposing the clean Fe(0 0 1) surface to 30 L (1 L = 1.0×10^{-6} Torr s) of molecular oxygen (partial pressure of 2 × 10^{-7} Torr, exposure time of 150 s) at 450 °C and then higher temperature annealing at 700 °C for excess oxygen removal from the surface [25–29].

The above described Fe(0 0 1)-*p*(1 × 1)O preparation was followed by the deposition of the organic molecules in a dedicated vacuum chamber by means of Knudsen effusion cells, each separately filled with an MTPP (M being Zn, Co) purchased from Merck. Before sublimation on Fe (0 0 1)-*p*(1 × 1)O, each cell was separately degassed in vacuum. The MTPPs were deposited at evaporation temperatures of about 300 °C, depending on a prior calibration of the effusion rate of each MTPP cell. Temperature controllers stabilize the crucible heating temperatures within 0.5 °C. The MTPP deposition rate was monitored by a quartz microbalance that enabled one to maintain a rate of about 1 Å min^{-1}. A complete monolayer coverage of both ZnTPP and CoTPP molecules corresponds to a thickness of about 3.06 Å [18,23]. All the films were grown with the substrate kept at room temperature.

2.2. Sample characterization

All samples were characterized by photoemission spectroscopy (PES) and LEED. PES utilized unmonochromatized radiation from an ultraviolet He I ($h\nu$ = 21.2 eV) lamp. All PES spectra have been subject to satellite peaks removal. Photoelectrons were collected in a 150 mm hemispherical electron analyzer (SPECS GmbH) [30], providing an overall (electron + photon) full width at half maximum (FWHM) energy resolution of 15 meV. LEED was performed with a commercial apparatus (Physical Electronics Inc.) equipped with a beam shutter. LEED images were taken at an incident beam energy of 55 eV after the spectroscopic characterizations, by exposing the sample to the electron beam for a few seconds. LEED patterns observed in the experiments have been corroborated with simulated LEED patterns produced by the software LEEDpat [31].

3. Results and discussion

3.1. Homogeneous MTPP monolayers on Fe(0 0 1)-p(1 × 1)O

For the sake of clarity, we start our discussion by considering first the case of a single type of MTPP molecule deposited onto the substrate (homogeneous deposition). The LEED patterns for ZnTPP and CoTPP monolayers on Fe(0 0 1)-*p*(1 × 1)O are reported in Fig. 1 (i) and (ii) respectively. In particular, Fig. 1 (i) shows the characteristic molecular reconstruction of a ZnTPP monolayer on Fe(0 0 1)-*p*(1 × 1)O: the black circled diffraction spots correspond to the reciprocal lattice of the underlying Fe(0 0 1)-*p*(1 × 1)O substrate, while the others (a subset of which is shown circled in yellow) give rise to the (5 × 5) surface reconstruction. A (5 × 5)R37° reconstruction is shown in Fig. 1 (ii) for the CoTPP monolayer (with some of the relative diffraction spots shown circled in pink). Both these patterns have also been reported in [25]. A detailed modeling of the molecular assemblies in the direct lattice space and the corresponding simulated LEED pattern for both cases are reported in Supplementary Information A.

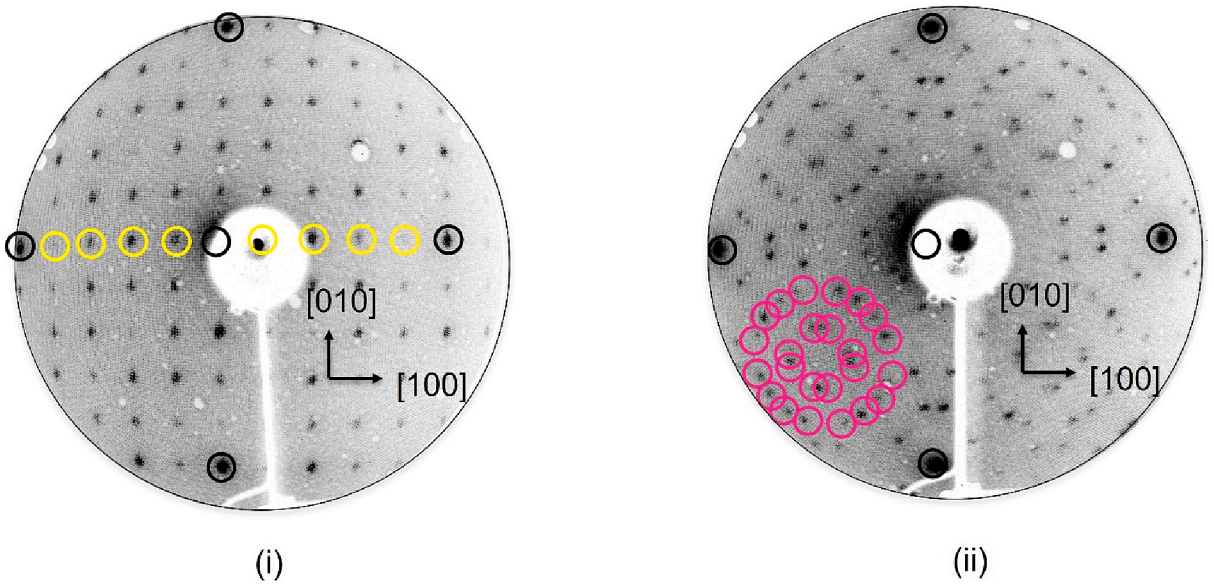

Fig. 1. (color online) LEED images obtained at 55 eV beam voltage for: **(i)** (5 × 5) surface reconstruction of 1 ML ZnTPP on Fe(001)-*p*(1 × 1)O (with some of the diffraction spots highlighted in yellow); and **(ii)** (5 × 5)R37° surface reconstruction of 1 ML CoTPP on Fe(001)-*p*(1 × 1)O (with some of the diffraction spots highlighted in pink). The 4 dark corner spots and the one in the middle are diffraction spots from the underlying Fe(001)-*p*(1 × 1)O substrate.

Further information on the homogeneous depositions are obtained by PES, as reported in Fig. 2. Indeed, given its rather shallow information depth (about 0.5 nm, according to Ref. [32]), the PES technique is particularly sensitive to changes in the O 2p peak contribution of the Fe (001)-*p*(1 × 1)O observed in the valence band region [33,34]. This peak completely disappears as soon as 1 ML coverage of MTPP molecules is reached. Fig. 2 (i) and (ii) show the PES characterizations for ZnTPP and CoTPP as a function of the deposited coverages. The peak at 4.3 eV binding energy (BE) indicates the characteristic O 2p spectral feature, which we attribute to the progressively buried Fe(001)-*p*(1 × 1)O substrate. Both the ZnTPP and CoTPP monolayers develop a wetting layer where molecules spread over the substrate rather than forming islands. This is evident from the complete disappearance of the O 2p peak at the 1 ML coverage, likely due to the combined effect of electronic modifications occurring at the interface and the distortion of the photoemission signal by scattering by the molecular layer, as discussed in our previous work [24]. We note that, if the development of the monolayer were island-like, the O 2p peak signal from the uncovered substrate would be visible even at and above 1 ML coverage. This is also confirmed by the fact that, at 1 ML coverage, STM images exclude the presence of any area where the bare substrate is visible [17,23]. At larger coverages, the LEED pattern fades away and specific modifications occur in the spectroscopic features from the molecular film, as shown in Ref. [29].

3.2. Heterogeneous ZnTPP - CoTPP monolayers on Fe(001)-p(1 × 1)O

3.2.1. Photoemission analysis

As mentioned in the Introduction section, heterogeneous M_1TPP + M_2TPP monolayers (M_1 being Zn or Co and M_2 being Co or Zn, respectively) were grown sequentially at room temperature by depositing *x* ML of M_1TPP on Fe(001)-*p*(1 × 1)O followed by (1-*x*) ML of M_2TPP, where $x \leq 1$. Furthermore, in another set of depositions, nominally equal amounts of ZnTPP and CoTPP were grown in co-deposition. A list of all

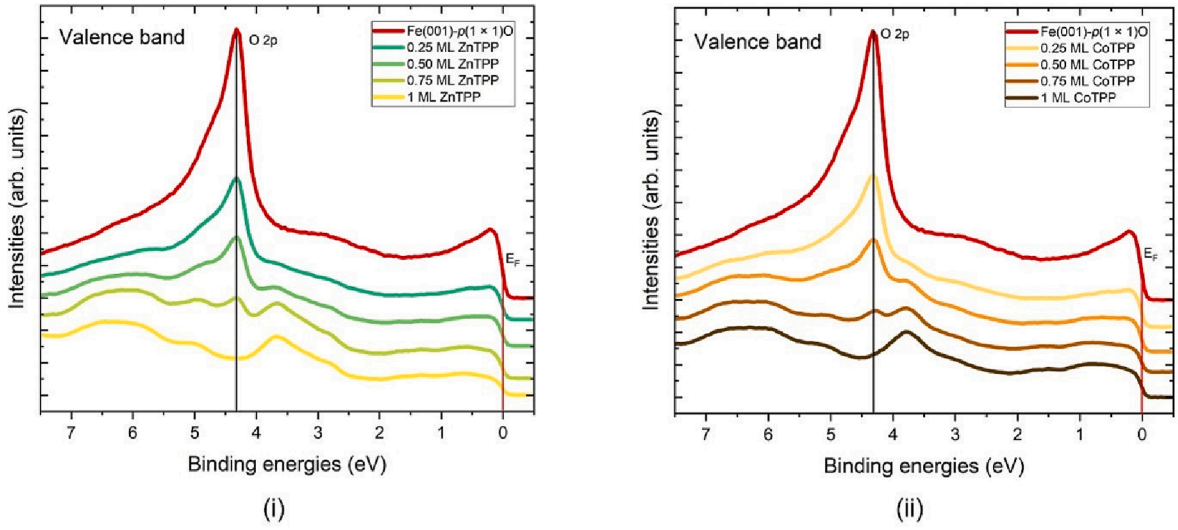

Fig. 2. (color online) PES spectra of MTPP films deposited at incremental coverages on Fe(001)-*p*(1 × 1)O: **(i)** ZnTPP **(ii)** CoTPP, where PES utilized radiation from an ultra-violet He I ($h\nu$ = 21.2 eV) source.

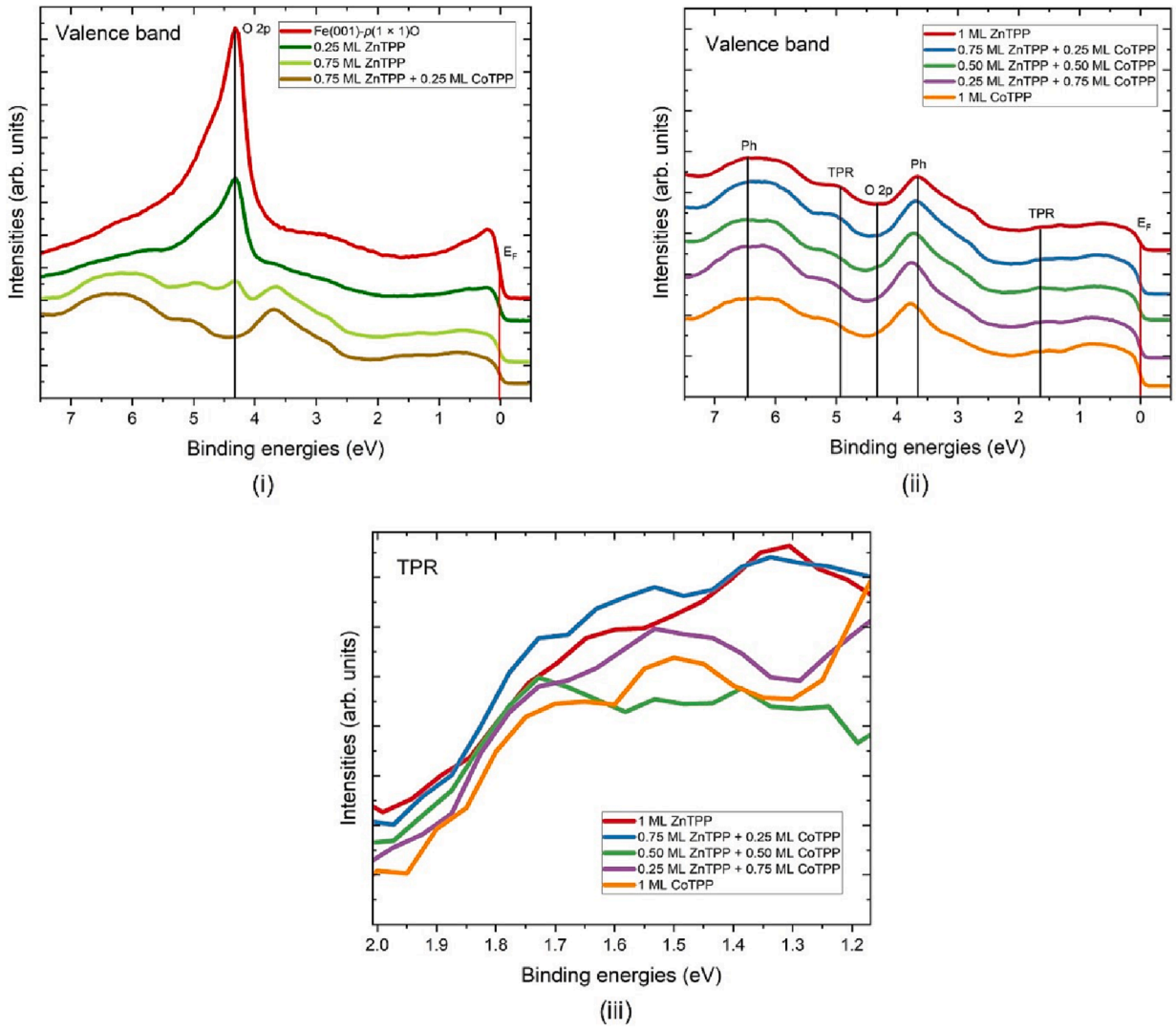

Fig. 3. (color online)PES spectra of MTPP depositions on Fe(0 0 1)-$p(1 \times 1)$O: **(i)** transition from homogeneous to heterogeneous ZnTPP – CoTPP monolayer, **(ii)** heterogeneous ZnTPP - CoTPP depositions, where ZnTPP is deposited first followed by CoTPP, and **(iii)** first TPR at about 1.6 eV or HOMO features as measured by PES. PES utilized radiation from an ultra-violet He I ($h\nu = 21.2$ eV) source.

the samples prepared and studied is reported as Table S1 in Supplementary Information B.

The influence of the presence of different types of molecules in the formation of the organic overlayer, for which we have no unambiguous evidence that ZnTPP and CoTPP mix, has been investigated by analyzing PES data for the heterogeneous MTPP depositions reported in Fig. 3. First of all, as clearly shown in Fig. 3 (i), we find, also in this case, the reduction of the O 2p peak signal as in the case of the homogeneous depositions (Fig. 2), pointing towards a similar growth mode. This indicates that MTPP domains prefer to be spatially distributed over the substrate spreading like a wetting layer and deposited on available free substrate region rather than accumulating on top of one another like in island formation, in case of both homogeneous as well as heterogeneous MTPP depositions. Thus a 1 ML of MTPP can be constructed as the deposition of x ML of $M_1TPP + (1\text{-}x)$ ML of M_2TPP: this will be taken as a starting point in the following section for analyzing LEED data from heterogeneous deposited films.

Along with reduction of the substrate contribution, upon increasing the MTPP coverage, spectral features characteristic of the organic molecule develop in the valence band region. Such features are highlighted in Fig. 3 (ii) for the ZnTPP–CoTPP heterogeneous monolayers for different values of the composition x, where ZnTPP is deposited first, followed by CoTPP, and a comparison is made with the respective homogeneous ZnTPP and CoTPP monolayers. In agreement with the other data available from the literature [18,21,35,36], the valence band region predominantly shows the influence of the main tetrapyrrole ring (TPR) at 1.6 eV and 5.0 eV and the phenyl (Ph) groups of the MTPP molecules at 3.7 eV and 6.5 eV. The first TPR feature after the Fermi level (E_F) at 1.6 eV also corresponds to the highest occupied molecular orbital (HOMO) level of the porphyrin molecule (detailed features shown in Fig. 3 (iii)). Slight energy shifts towards higher BEs in the peak positions at the Ph position of 3.7 eV and the TPR position of 5.0 eV are observed. Nevertheless, the molecular features are preserved in the case of heterogeneous depositions as well. A more detailed analysis of the ZnTPP and CoTPP valence structures, in our case, requires a careful subtraction of features arising from Fe, as opposed to porphyrin films deposited on noble metal substrates [36–38]. For such an analysis, dealing with the possible occupation of additional states close to E_F, the reader is referred to our previous work [21].

3.2.2. *LEED analysis: Superposition criterion*

As discussed above, the PES data suggests the possibility of building a single organic monolayer as the linear superposition of x ML M_1TPP and $(1\text{-}x)$ ML of M_2TPP. An interesting question is then if this linear

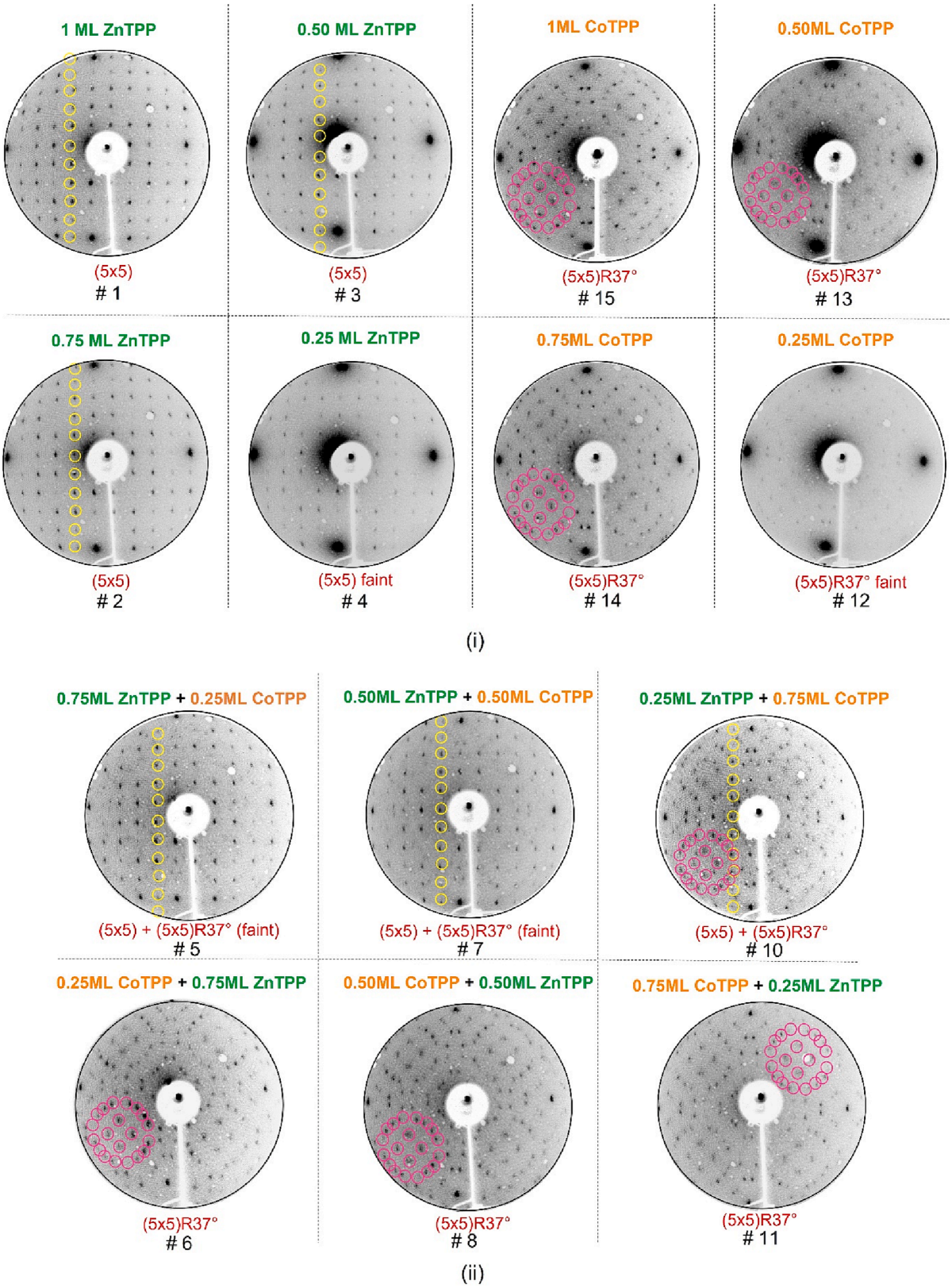

Fig. 4. (color online) LEED images obtained at 55 eV beam energy for the samples listed in Table S1 of Supplementary Information B: **(i)** homogeneous depositions as a function of film coverages, and **(ii)** heterogeneous $M_1TPP + M_2TPP$ depositions. The black circled diffraction spots are due to the underlying Fe(001)-$p(1 \times 1)$O substrate, the highlighted yellow circles exhibit (5×5) ordering of ZnTPP molecules, and the highlighted pink circles exhibit (5×5)R37° ordering of CoTPP molecules.

superposition can be observed in diffraction patterns as well. Fig. 4 shows the LEED patterns for all the samples (with the numbers referring to Table S1 reported in Supplementary Information B. Samples reported in Fig. 4 (i), i.e. single molecule films have various coverages: 0.25 ML, 0.50 ML, 0.75 ML and 1 ML. These have been used to interpret the heterogeneous films whose LEED patterns are shown in Fig. 4 (ii). In particular, the deposition sequence between ZnTPP and CoTPP has been found to be of significant importance as will be described as follows.

From the heterogeneous ZnTPP - CoTPP depositions shown in Fig. 4 (ii), we observe that samples (please refer to Table S1 in Supplementary Information B) labeled #5, #7 and #10 show LEED patterns whose interpretation can be quantitatively based on a criterion of superposition. For example, sample #5, which is a 0.75 ML ZnTPP deposition followed by a 0.25 ML CoTPP deposition, shows a LEED pattern that seems to be simply a linear combination of the diffraction patterns observed in samples #2 and #12. In this LEED image, a faint rotated (5 × 5)R37° pattern superimposes an otherwise bright straight (5 × 5) pattern. A similar linear combination is found in the case of sample #7, which is a 0.50 ML ZnTPP deposition followed by a 0.50 ML CoTPP deposition. The final LEED image shows a combination of a straight (5 × 5) and a faint rotated (5 × 5)R37° pattern, which seems to be the superposition of the patterns shown by samples #3 (pure 0.50 ML ZnTPP film) and #13 (pure 0.50 ML CoTPP film). The criterion of superposition has also been found to be valid when 0.75 ML of CoTPP is deposited on a pre-covered substrate with 0.25 ML of ZnTPP (sample #10). As seen from the LEED image corresponding to sample #10 in Fig. 4 (ii), CoTPP molecules retain their characteristic (5 × 5)R37° pattern which results in a clear mixed and bright straight (5 × 5) and rotated (5 × 5)R37° pattern. A detailed modeling of the molecular assemblies in the direct lattice space and the corresponding simulated LEED pattern for this case is reported in Supplementary Information C.1.

3.2.3. *LEED analysis: CoTPP pre-coverage and triggering effect*

If we look at the LEED pattern of sample #6 in Fig. 4 (ii), which is a heterogeneous porphyrin film obtained by a first deposition of 0.25 ML CoTPP, followed by 0.75 ML of ZnTPP, instead of observing a clear bright straight (5 × 5) ordering due to a relatively huge amount of ZnTPP, we actually observe the presence of only the (5 × 5)R37° pattern, suggesting that ZnTPP molecules prefer to continue the molecular ordering created by the initial CoTPP deposition. A naïve model of the molecular assemblies in the direct lattice space for this case is reported in Supplementary Information C.2. The same phenomenon is observed every time that CoTPP is pre-deposited on the substrate surface (samples #6, #8 and #11), indicating that once the sequence of deposition in the heterogeneous porphyrin films is changed, the criterion of superposition no longer holds valid.

The dominant effect of CoTPP in driving the final LEED pattern is also evident in co-deposition conditions. Fig. 5 (i) shows the LEED pattern of a simultaneous deposition of half a monolayer of ZnTPP molecules and half a monolayer of CoTPP molecules (sample #9). Instead of observing a mixed pattern what we observed was only a (5 × 5)R37° pattern. A naïve model of the real space (Fig. 5 (ii)) demonstrates this triggering effect of CoTPP, despite both ZnTPP and CoTPP molecules arriving on the substrate at the same time.

As a naïve interpretation of the above phenomena observed and the CoTPP dominance/triggering effect, we speculate to consider differences in the porphyrin diffusion on a surface. Generally speaking, some factors are crucial in this process, such as: (i) molecule–substrate interaction [39–41], (ii) inter-molecular coupling through Van der Waals, electrostatic, CH-π and/or π-π interactions [42], and (iii) structural and electronic properties of the molecule, which can depend on the type of central metal ion [43]. In our case, previous investigations on different porphyrin layers grown on the passivated iron surface reveal a general weak porphyrin-iron interaction due to the oxygen passivation treatment of the substrate [24,44,45]. As a consequence, the molecular diffusion might be influenced by the other two factors. We speculate that the pre-deposited CoTPPs with (5 × 5)R37° molecular assembling offer domains accessible to the arriving ZnTPP molecules on their diffusion paths across the substrate surface possibly due to ZnTPPs having a different diffusivity as well as the ZnTPP - CoTPP attractive interactions being preferred over the ZnTPP - ZnTPP ones. Under these conditions, the pre-existing (5 × 5)R37° or CoTPP domains spread due to the

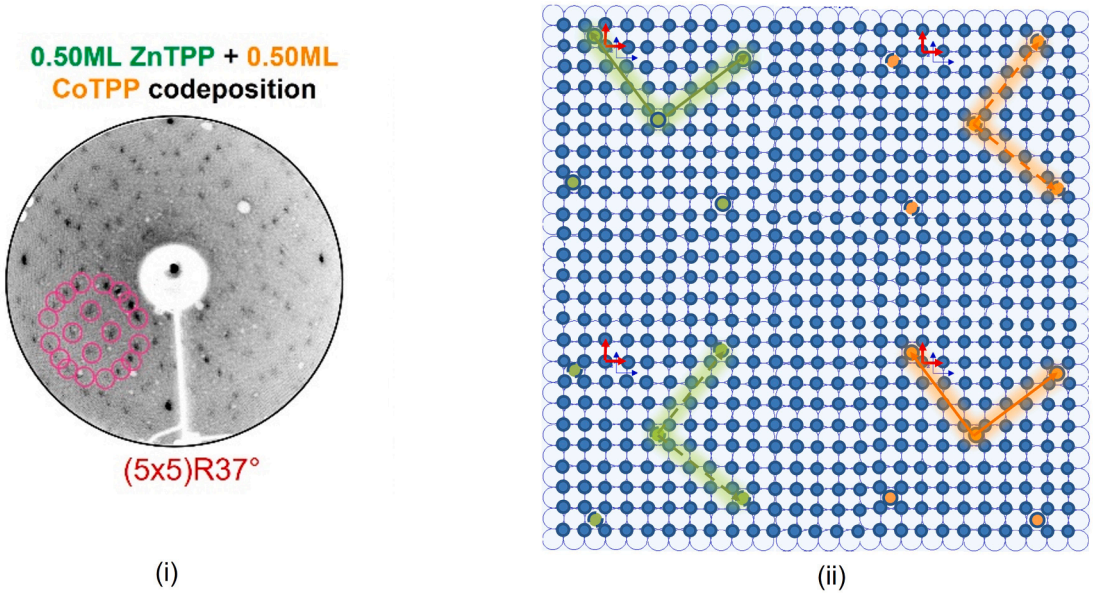

Fig. 5. (color online) (i) LEED image of (5 × 5)R37° surface reconstruction of the 0.50 ML ZnTPP + 0.50 ML CoTPP co-deposited sample, obtained at 55 eV beam energy, and **(ii)** a naïve model of an Fe *bcc* (0 0 1) plane top view showing the direct lattice space, where the molecules distribution can be envisaged in its simplest form. The ZnTPP molecules are shown occupying half of the space with a (5 × 5) assembling (green dots signify Zn^{2+} central metal ions) while the rest is filled with CoTPP molecules with their (5 × 5)R37° ordering (orange dots signify Co^{2+} central metal ions). The rest of the molecular skeleton is not displayed here for simplicity. The red lattice vector directions represent the O atoms (deep blue spheres) spacing, which are located on the four-fold hollow positions of the Fe lattice (Fe atoms represented by light blue spheres). The highlighted green and orange lattice vectors correspond to Zn^{2+} and Co^{2+} ion spacings as shown in Supplementary Information A.

adherence of ZnTPP molecules on the border of such domains and therefore the final LEED pattern shows a single (5 × 5)R37° diffraction image. Conversely, on a pre-deposited ZnTPP substrate surface, the arriving CoTPP molecules are not able to expand the pre-existing ZnTPP domains with (5 × 5) molecular assembling as well as the CoTPP – CoTPP attractive interactions being preferred over the ZnTPP – CoTPP attractive interactions and the former promoting the growth of separate CoTPP domains with (5 × 5)R37° molecular assembling. Therefore, in this case, the final LEED pattern is simply a linear superposition of the (5 × 5) pattern as contributed by the pre-existing ZnTPP domains and the (5 × 5)R37° pattern as contributed by the subsequently newly formed CoTPP domains.

4. Conclusions

Heterogeneous organic films are of crucial interest for application in organic electronic devices and, consequently, there is a general interest in improving the understanding of organic molecular self-assembling on surfaces. In this work, we studied both homogeneous ZnTPP (CoTPP) monolayers as well as heterogeneous ZnTPP - CoTPP monolayers deposited on Fe(001)-*p*(1 × 1)O substrate. PES was employed to monitor the substrate coverage during sublimation of homogeneous and heterogeneous films. In both cases, PES suggests an initial layer-by-layer growth mode and the possibility to obtain a monolayer composed of the two porphyrin molecules. The organic film crystallinity was studied by LEED. Homogeneous ZnTPP (CoTPP) films are characterized by a clear (5 × 5) [(5 × 5)R37°] reconstruction. A pre-deposited ZnTPP sub-monolayer film, followed by a CoTPP deposition (to a final coverage of nominal 1 ML), reveals a complex LEED diffraction pattern that can be interpreted in terms of a linear superposition of the (5 × 5) and the (5 × 5)R37° patterns. Surprisingly, a sub-monolayer pre-deposition of CoTPP molecules drives the subsequent ZnTPP deposition (final coverage of nominal 1 ML) to show a single (5 × 5)R37° LEED pattern. Our results put in evidence unexpected differences in the growth of heterogeneous organic films in terms of the sequence of deposition. A tentative interpretation of the results suggests a difference in surface diffusion for the two MTPPs. In our opinion, further experimental data, for instance investigating the role of the temperature after the growth of the films, as in temperature-programmed desorption, and developing a theoretical analysis pertaining to molecules diffusion on passivated metal surfaces is desirable for a better comprehension of heterogeneous organic film growth.

CRediT authorship contribution statement

Isheta Majumdar: Conceptualization, Methodology, Formal analysis, Investigation, Writing – original draft, Writing – review & editing. **Francesco Goto:** Methodology, Investigation. **Alberto Calloni:** Conceptualization. **Guglielmo Albani:** Methodology. **Lamberto Duò:** Project administration. **Marco Finazzi:** Writing – review & editing. **Franco Ciccacci:** Writing – review & editing, Supervision. **Gianlorenzo Bussetti:** Conceptualization, Supervision, Funding acquisition.

Declaration of Competing Interest

The authors declare that they have no known competing financial interests or personal relationships that could have appeared to influence the work reported in this paper.

Data availability

Data will be made available on request.

Acknowledgement

The present work has been undertaken under the project MOXOPIF – METAL OXIDE/ORGANIC PASSIVATED INTERFACES: IMPLICATIONS FOR ORGANIC ELECTRONICS with project code (CUP) D43C22004190001 under Ministero dell'Università e della Ricerca (MUR) grant ID no. SOE_0000076. The Marie Skłodowska-Curie Action (MSCA) Seal of Excellence Individual Fellowship 2020 project with project code (CUP) D45F21005290001 under grant no. UA.A.RRR.DFIS. PAMM.STUD.BGP1VARI01 is also acknowledged.

Appendix A. Supplementary data

Supplementary data to this article can be found online at https://doi.org/10.1016/j.apsusc.2023.157807.

References

[1] N. Xin, J. Guan, C. Zhou, X. Chen, C. Gu, Y. Li, M.A. Ratner, A. Nitzan, J. F. Stoddart, X. Guo, Concepts in the design and engineering of single-molecule electronic devices, Nat. Rev. Phys. 1 (2019) 211–230.
[2] C. K. Chiang, C. R. Jr. Fincher, Y. W. Park, A. J. Heeger, H. Shirakawa, E. J. Louis, S. C. Gau, A. G. MacDiarmid, Electrical conductivity in doped polyacetylene, Phys. Rev. Lett. 40 (1978) 1472.
[3] G. Lanzani, Materials for bioelectronics: Organic electronics meets biology, Nat. Mater. 13 (8) (2014) 775–776.
[4] H. Xu, R. Chen, Q. Sun, W. Lai, Q. Su, W. Huang, X. Liu, Recent progress in metal-organic complexes for optoelectronic applications, Chem. Soc. Rev. 43 (2014) 3259–3302.
[5] G. Chidichimo, F. Luigi, Organic solar cells: Problems and perspectives, Int. J. Photoenergy (2010), https://doi.org/10.1155/2010/123534.
[6] W. Auwaerter, K. Seufert, F. Bischoff, D. Ecija, S. Vijayaraghavan, S. Joshi, F. Klappenberger, N. Samudrala, J.V. Barth, A surface-anchored molecular four-level conductance switch based on single proton transfer, Nat. Nanotechnol. 7 (1) (2011) 41–46.
[7] A.M. Steiner, F. Lissel, A. Fery, J. Lauth, M. Scheele, Prospects of coupled organic-inorganic nanostructures for charge and energy transfer applications, Angew. Chem. Int. Ed. (2020), https://doi.org/10.1002/anie.201916402.
[8] A.M. Bagher, Comparison of organic solar cells and inorganic solar cells, Int. J. Sustain. Green Energy 3 (3) (2014) 53–58.
[9] S. Logothetidis, Flexible organic electronic devices: Materials, process and applications, Mater. Sci. Eng., B 152 (2008) 96–104.
[10] A.F. Aliaga, E. Coronado, Hybrid Interfaces in Molecular Spintronics, Chem. Rec. 18 (2018) 737–748.
[11] K.O. Legg, F. Jona, D.W. Jepsen, P.M. Marcus, Early stages of oxidation of the Fe (001) surface: Atomic structure of the first monolayer, Physical Review B 16 (12) (1977) 5271–5276.
[12] A. Picone, A. Brambilla, A. Calloni, L. Duo', M. Finazzi, F. Ciccacci, Oxygen-induced effects on the morphology of the Fe(001) surface in out-of-equilibrium conditions, Phys. Rev. B: Condens. 83 (2011) 235402.
[13] W. Dou, S. Huang, R.Q. Zhang, C.S. Lee, Molecule-substrate interaction channels of metal-phthalocyanines on graphene on Ni(111) surface, J. Chem. Phys. 134 (2011) 094705.
[14] A.O. Biroli, A. Calloni, A. Bossi, M.S. Jagadeesh, G. Albani, L. Duò, F. Ciccacci, A. Goldoni, A. Verdini, L. Schio, L. Floreano, G. Bussetti, Out-of-plane metal coordination for a true solvent-free building with molecular bricks: Dodging the surface ligand effect for on-surface vacuum self-assembly, Adv. Funct. Mater. 31 (2021) 2011008.
[15] G. Albani, M. Capra, A. Lodesani, A. Calloni, G. Bussetti, M. Finazzi, F. Ciccacci, A. Brambilla, L. Duò, A. Picone, Self-assembly of C_{60} on a ZnTPP/Fe(001)-*p*(1 × 1)O substrate: Observation of a quasi-freestanding C_{60} monolayer, Beilstein J. Nanotechnol. 13 (2022) 857–864.
[16] A. Picone, D. Gianotti, M. Riva, A. Calloni, G. Bussetti, G. Berti, L. Duò, F. Ciccacci, M. Finazzi, A. Brambilla, Controlling the electronic and structural coupling of C_{60} nano films on Fe(001) through oxygen adsorption at the interface, ACS Appl. Mater. Interfaces 8 (39) (2016) 26418–26424.
[17] A. Picone, D. Giannotti, A. Brambilla, G. Bussetti, A. Calloni, M. Rossella Yivlialin, L. Finazzi, F. Duò, A. Ciccacci, A. Goldoni, L.F. Verdini, Local structure and morphological evolution of ZnTPP molecules grown on Fe(001)-*p*(1 × 1)O studied by STM and NEXAFS, Appl. Surf. Sci. 435 (2018) 841–847.
[18] G. Bussetti, A. Calloni, R. Yivlialin, A. Picone, F. Bottegoni, M. Finazzi, Filled and empty states of Zn-TPP films deposited on Fe(001)-*p*(1×1)O, Beilstein J. Nanotechnol. 7 (2016) 1527–1531.
[19] A. Franco-Canellas, S. Duhm, A. Gerlach, F. Schreiber, Binding and electronic level alignment of π- conjugated systems on metals, Rep. Prog. Phys. 83 (2020) 066501.
[20] J. Michael Gottfried, Surface chemistry of porphyrins and phthalocyanines, Surf. Sci. Rep. 70 (2015) 259–379.
[21] A. Calloni, M.S. Jagadeesh, G. Bussetti, G. Fratesi, S. Achilli, A. Picone, A. Lodesani, A. Brambilla, C. Goletti, F. Ciccacci, L. Duò, M. Finazzi, A. Goldoni, A. Verdini, L. Floreano, Cobalt atoms drive the anchoring of Co-TPP molecules to the oxygen-passivated Fe(001) surface, Appl. Surf. Sci. 505 (2020) 144213.
[22] G. Bussetti, A. Calloni, M. Celeri, R. Yivlialin, M. Finazzi, F. Bottegoni, L. Duò, F. Ciccacci, Structure and electronic properties of Zn-tetra-phenyl-porphyrin single- and multi-layers films grown on Fe(001)-*p*(1 × 1)O, Appl. Surf. Sci. 390 (2016) 856–862.

[23] M.S. Jagadeesh, A. Calloni, A. Brambilla, A. Picone, A. Lodesani, L. Duò, F. Ciccacci, G. Bussetti, Room temperature magnetism of ordered porphyrin layers on Fe, Appl. Phys. Lett. 115 (2019) 082404.
[24] G. Fratesi, S. Achilli, A. Ugolotti, A. Lodesani, A. Picone, A. Brambilla, L. Floreano, A. Calloni, G. Bussetti, Nontrivial central-atom dependence in the adsorption of M-TPP molecules (M = Co, Ni, Zn) on Fe(001)-$p(1 \times 1)$O, Appl. Surf. Sci. 530 (2020) 147085.
[25] R. Bertacco, S. De Rossi, F. Ciccacci, High-quality Fe(001) single crystal films on MgO(001) substrates for electron spectroscopies, J. Vac. Sci. Technol., A 16 (1998) 2277.
[26] R. Bertacco, F. Ciccacci, Oxygen-induced enhancement of the spin-dependent effects in electron spectroscopies of Fe(001), Phys. Rev. B: Condens. Matter 59 (6) (1999) 4207–4210.
[27] A. Picone, G. Bussetti, M. Riva, A. Calloni, A. Brambilla, L. Duò, F. Ciccacci, M. Finazzi, Oxygen-assisted Ni growth on Fe(001): Observation of an "anti-surfactant" effect, Phys. Rev. B: Condens. Matter 86 (2012) 075465.
[28] A. Brambilla, A. Calloni, A. Picone, M. Finazzi, L. Duò, F. Ciccacci, X-ray photoemission spectroscopy investigation of the early stages of the oxygen aided Cr growth on Fe(001), Appl. Surf. Sci. 267 (2013) 141–145.
[29] A. Calloni, M.S. Jagadeesh, G. Albani, C. Goletti, L. Duò, F. Ciccacci, G. Bussetti, Ordered assembling of Co tetra phenyl porphyrin on oxygen-passivated Fe(001): From single to multilayer films, *FisMat 2019*, EPJ Web Conf. 230 (2020) 00014, https://doi.org/10.1051/epjconf/202023000014.
[30] G. Berti, A. Calloni, A. Brambilla, G. Bussetti, L. Duò, F. Ciccacci, Direct observation of spin-resolved full and empty electron states in ferromagnetic surfaces, Rev. Sci. Instrum. 85 (2014) 073901.
[31] K. E. Hermann, M. A. Van Hove, LEEDpat4, http://www.fhi-berlin.mpg.de/KHsoftware/LEEDpat/index.html.
[32] M.P. Seah, W.A. Dench, Quantitative electron spectroscopy of surfaces: A standard data base for electron inelastic mean free paths in solids, Surf. Interface Anal. 1 (1979) 2–11.
[33] A. Calloni, G. Fratesi, S. Achilli, G. Berti, G. Bussetti, A. Picone, A. Brambilla, P. Folegati, F. Ciccacci, L. Duò, Combined spectroscopic and *ab initio* investigation of monolayer-range Cr oxides on Fe(001): The effect of ordered vacancy superstructure, Phys. Rev. B: Condens. Matter 96 (2017) 085427.
[34] A. Clarke, N.B. Brookes, P.D. Johnson, M. Weinert, B. Sinković, N.V. Smith, Spin-polarized photoemission studies of the adsorption of O and S on Fe(001), Phys. Rev. B: Condens. Matter 41 (14) (1990) 9659–9667.
[35] S. Rangan, S. Katalinic, R. Thorpe, R.A. Bartynski, J. Rochford, E. Galoppini, Energy level alignment of a zinc(II) tetraphenylporphyrin dye adsorbed onto TiO2 (110) and ZnO(11 $\bar{2}$ 0) surfaces, J. Phys. Chem. C 114 (2010) 1139–1147.
[36] D.A. Duncan, P.S. Deimel, A. Wiengarten, M. Paszkiewicz, P. Casado Aguilar, R. G. Acres, F. Klappenberger, W. Auwärter, A.P. Seitsonen, J.V. Barth, F. Allegretti, Bottom-up fabrication of a metal-supported oxo−metal porphyrin, J. Phys. Chem. C 123 (2019) 31011–31025.
[37] G. Di Santo, C. Castellarin-Cudia, M. Fanetti, B. Taleatu, P. Borghetti, L. Sangaletti, L. Floreano, E. Magnano, F. Bondino, A. Goldoni, Conformational adaptation and electronic structure of 2H-tetraphenylporphyrin on Ag(111) during Fe metalation, J. Phys. Chem. C 115 (2011) 4155–4162.
[38] T. Lukasczyk, K. Flechtner, L.R. Merte, N. Jux, F. Maier, J.M. Gottfried, H.-P. Steinrück, Interaction of cobalt(II) tetraarylporphyrins with a Ag(111) surface studied with photoelectron spectroscopy, J. Phys. Chem. C 111 (2007) 3090–3098.
[39] W. Auwaerter, F. Klappenberger, A. Weber-Bargioni, A. Schiffrin, T. Strunskus, C. h. Woell, Y. Pennec, A. Riemann, J.V. Barth, Conformational adaptation and selective adatom capturing of tetrapyridyl-porphyrin molecules on a copper(111) surface, J. Am. Chem. Soc. 129 (36) (2007) 11279–11285.
[40] J. Brede, M. Linares, S. Kuck, J. Schwoebel, A. Scarfato, S.-H. Chang, G. Hoffman, R. Wiesendanger, R. Lensen, P.H.J. Kouwer, J. Hoogboom, A.E. Rowan, M. Broering, M. Funk, S. Stafstrom, F. Zerbetto, R. Lazzaroni, Dynamics of molecular self-ordering in tetraphenyl porphyrin monolayers on metallic substrates, Nanotechnology 20 (2009) 275602.
[41] G. Rojas, X. Chen, C. Bravo, J.-H. Kim, J.-S. Kim, J. Xiao, P.A. Dowben, Y. Gao, X. C. Zeng, W. Choe, A. Enders, Self-assembly and properties of nonmetalated tetraphenyl-porphyrin on metal substrates, J. Phys. Chem. Phys. Rev. B: Condens. Matter C 114 (2010) 9408–9415.
[42] J. Brede, M. Linares, R. Lensen, A.E. Rowan, M. Funk, M. Broering, G. Hoffmann, R. Wiesendanger, Adsorption and conformation of porphyrins on metallic surfaces, J. Vac. Sci. Technol. B 27 (2009) 799.
[43] F. Rosei, M. Schunack, Y. Naitoh, P. Jiang, A. Gourdon, E. Laegsgaard, I. Stensgaard, C. Joachim, F. Besenbacher, Properties of large organic molecules on metal surfaces, Prog. Surf. Sci. 71 (2003) 95–146.
[44] G. Albani, A. Calloni, M.S. Jagadeesh, M. Finazzi, L. Duò, F. Ciccacci, G. Bussetti, Interaction of ultra-thin CoTPP films on Fe(001) with oxygen: Interplay between chemistry, order, and magnetism, J. Appl. Phys. 128 (2020) 035501.
[45] G. Albani, A. Calloni, A. Picone, A. Brambilla, M. Capra, A. Lodesani, L. Duò, M. Finazzi, F. Ciccacci, G. Bussetti, An in-depth assessment of the electronic and magnetic properties of a highly ordered hybrid interface: The case of nickel tetraphenyl-porphyrins on Fe(001)–$p(1 \times 1)$O, Micromachines 12 (2021) 191.